geosciences

MDPI

Review

Bridging the Gap between Long–Term Orogenic Evolution (>10 Ma Scale) and Geomorphological Processes That Shape the Western Alps: Insights from Combined Dating Approaches

Yann Rolland [1,2,*], Antonin Bilau [1,2], Thibaut Cardinal [3], Ahmed Nouibat [2], Dorian Bienveignant [2], Louise Boschetti [1,2], Stéphane Schwartz [2] and Matthias Bernet [2]

[1] Departement Sciences de la Terre, Université Savoie Mont Blanc, CNRS, Edytem, 73370 Le Bourget-du-Lac, France
[2] Université Grenoble Alpes, Université Savoie Mont Blanc, CNRS, IRD, ISTerre, 38000 Grenoble, France
[3] Observatoire de la Côte d'Azur, Université Côte d'Azur, CNRS, IRD, Géoazur, 250 Rue Albert Einstein, Sophia Antipolis, 06560 Valbonne, France
* Correspondence: yann.rolland@univ-smb.fr

Abstract: Constraining the relative roles of erosion and tectonics in the evolution of mountain belts is a challenging scientific goal. In this review article on the Western Alps, we show how it becomes possible to "bridge the gap" between the long–term (>Ma) orogenic evolution controlled by tectonics and exhumation processes and the recent geomorphological evolution that is accessible on an annual–decadal basis. Advances in mineral dating that have grown in relation to deformation in the ductile and brittle crustal fields have allowed us to constrain the evolution of deformation through time and depth. A drastic change from early collision, dominated by rapid underthrusting of the European plate, to a more stagnant syn–collisional tectonic context is documented since about 26–20 Ma by syn–kinematic phengites and vein–hosted monazites along the Alpine arc. The overall dextral kinematic context is accompanied by local extensional domains in the Simplon and High Durance Valley. Activation of the Simplon ductile fault is documented from 20 Ma, whereas the High Durance extensional system commenced after 10 Ma. The application of cosmogenic nuclide dating of incised river gorges demonstrates that the erosion pattern of the Western Alps follows a different evolution within the valleys dominated by upstream glacial erosion than in peripheral watersheds devoid of glaciers. The very low peripheral incision is found to be similar to the vertical GPS signal, suggesting equilibrium of tectonic uplift and incision, whereas the glacial–dominated valleys exhibit significantly increased and transient river incision during interglacials and a constant ongoing tectonic regime.

Keywords: alps; orogens; geochronological methods; erosion; tectonics

Citation: Rolland, Y.; Bilau, A.; Cardinal, T.; Nouibat, A.; Bienveignant, D.; Boschetti, L.; Schwartz, S.; Bernet, M. Bridging the Gap between Long–Term Orogenic Evolution (>10 Ma Scale) and Geomorphological Processes That Shape the Western Alps: Insights from Combined Dating Approaches. *Geosciences* **2022**, *12*, 393. https://doi.org/10.3390/geosciences12110393

Academic Editors: M. Scott Harris, Niki Evelpidou, Charalampos Fassoulas and Jesus Martinez-Frias

Received: 26 August 2022
Accepted: 11 October 2022
Published: 25 October 2022

1. Introduction

The Alpine belt has been presented either as a mountain belt in which the relief is no longer sustained by tectonic motions (e.g., [1]), or as a tectonically active system in which tectonic forces contribute to maintain it [2,3]. As in many other orogens, the temporal evolution of deformation, surface uplift and rock cooling has been mainly investigated through thermochronology (e.g., [4–9]). The thermochronological approach has, however, the disadvantage that direct relationships of apparent cooling ages to geological structures and kinematics are often missing (e.g., [10]). For this reason, debate is ongoing on the use of thermochronological data to infer erosion rates and infer the role of tectonic structures in the active evolution of mountain belts [10–12]. In order to relate ages to tectonic displacements, it is possible to use minerals that grow in relation to deformation, such as micas and illites, along the stretching lineation direction of shear zones (e.g., [13–17]) or monazites in clefts [18–23]. Most notably, the Alpine orogen is a great example of a weakly deformed

region in which establishing the relative contributions of tectonic motions and climate in shaping the mountain belt is especially challenging. Based on thermochronological mapping and inverse methods [11,24], Champagnac et al. [25] propose that mountain building is mainly controlled by erosion related to climate change in the last 5 Ma. However, such studies are mainly based on bedrock and/or detrital thermochronological data, which give constraints on exhumation rates on Ma time scales. However, such data do not provide direct information on the timing of tectonic motion of specific faults zones, and thus it remains difficult to be conclusive about the contribution of fault systems to the recent evolution of a given mountain belt, especially when the tectonic motions are slow (<1 mm·yr^{-1}) and are most likely hindered by erosion (from 0.3–0.5 in general to >1 mm·yr^{-1} locally, in the Alps, [26]). Pin–pointing the tectonic history of fault systems in the last Myrs is thus important to give insights into their activity during the course of past glaciations and provide some information on their seismic risk potential (e.g., [27–29]). In order to fulfill this goal, it is necessary to obtain direct ages of fault motions, which remains challenging in the recent geological record [30,31]. In the present day, GPS–based studies can be used to detect horizontal and vertical motion gradients along fault systems, but for slow tectonics this will require a very dense network and long–term (>20 yr) analysis (e.g., [32–34]).

In this paper, we present a compilation of recent geochronological data on the Western Alpine belt, with emphasis on syn–kinematic minerals which crystallized in faults, shear zones and clefts (white mica, allanite, monazite, calcite) and on cosmogenic nuclide dating of the incision. These data unravel the ductile–to–brittle history of the Alpine arc and show that the observable present–day transcurrent tectonic motions initiated at ca. 26 to 20 Ma along the Alpine arc. Apatite Fission Track (AFT) data obtained in the footwall of the Penninic Front [5,35] show that this domain has been exhumed since at least 10 Ma, while AFT data acquired in the hanging wall are older, around 20 Ma [5]. Later, brittle extension along the High Durance Extensional system from ca. 5 Ma has been highlighted by calcite U/Pb dating [36]. Finally, active evolution of the belt highlighted by Cosmic Ray Exposure (CRE) dating allows constraining the last 80 kyr–incision and surface uplift history. Such a combination of data may allow the shedding of new light on tectonic and geomorphologic processes over <5 Ma time scales in slow, active, orogenic domains.

1.1. Recent (<20 Ma) and Active Tectonic Motions along the Penninic Line

Geophysical data show deformation at low strain rates in the Western Alps attributed to belt–parallel extension (e.g., [37,38]), and ongoing slow–rate rotation of the Apulian Plate mainly accommodated along the Penninic Line (e.g., [39–42]; Figure 1). Along the Alpine arc, the distribution of seismicity is diffuse (e.g., [3]). Seismic activity lies mostly in the hanging wall of the Penninic Line Fault in the Central Alps, whereas it is more spread out in the SW Alps, with seismicity crossing the Penninic Line along the Durance Extensional fault system [43]. Seismicity tends to cluster along (1) the internal part of the Penninic Line, with widespread extensional and transcurrent focal mechanisms and (2) somehow at the exterior of the chain along some oblique crustal lineaments with a combination of compressional and transcurrent focal mechanisms [38,44].

The Penninic Line is thus a good example of a major fault system, the ongoing activity of which is shown by the seismicity. However, the presence of significant fault motions remains debated. A first input from thermochronology shows that the Penninic Line has clearly been active in recent geological history (<20 Ma), as emphasized by fission–track dating undertaken on both sides of this fault (e.g., [5,45,46]; Figure 2). Offset is well documented along the Simplon normal fault, which is a local extensional domain connecting two dextral faults (Figure 1), and is clearly documented from 20 to 5 Ma (see compilations in [15,47,48]; Figure 2). For the younger fault history, apatite fission–track ages younger than 4 Ma, but also older than 6 Ma, occur on both sides of the Penninic Line, which makes it difficult to identify a fault motion on the sole basis of thermochronology. Based on field studies, several authors [46,49,50] find no significant post–Miocene motion

of the Penninic Line of any sense (normal or reverse). However, several other studies, especially in the SW Alps, suggest a continuous, though moderate, tectonic activity along the Penninic Line until the present day due to the similarity of past and active deformation patterns ([27,28,44,51]; Figure 3). Nonetheless, it still remains difficult to provide insights into the continuous activity of a given fault over the last several Myrs, during exhumation through low temperatures (<100 °C), because few markers of tectonic motion suitable for dating exist. A first line of evidence comes from the offset of glacial morphologies such as in the Argentera–Mercantour Massif (Figure 4; [27,28,52]). In this domain of the Alps, seismicity is significantly higher and shows identical stress directions (focal mechanisms) as the paleo–stress derived from fault–striae data measured in the field [27,28,43,51,53]. This similarity suggests that the present–day tectonics of the SW Alps are more or less identical to the long–term tectonic motions at the scale of <1 Ma (morphologies offset, [52]) and <10 Ma (brittle deformation, [28,30]). In the SW Alps, these dextral faults show signs of recent activity along the rim of the Argentera–Mercantour and south to the French Riviera along the Nice Arc [30,51], where Pliocene conglomerates are verticalized and deformed.

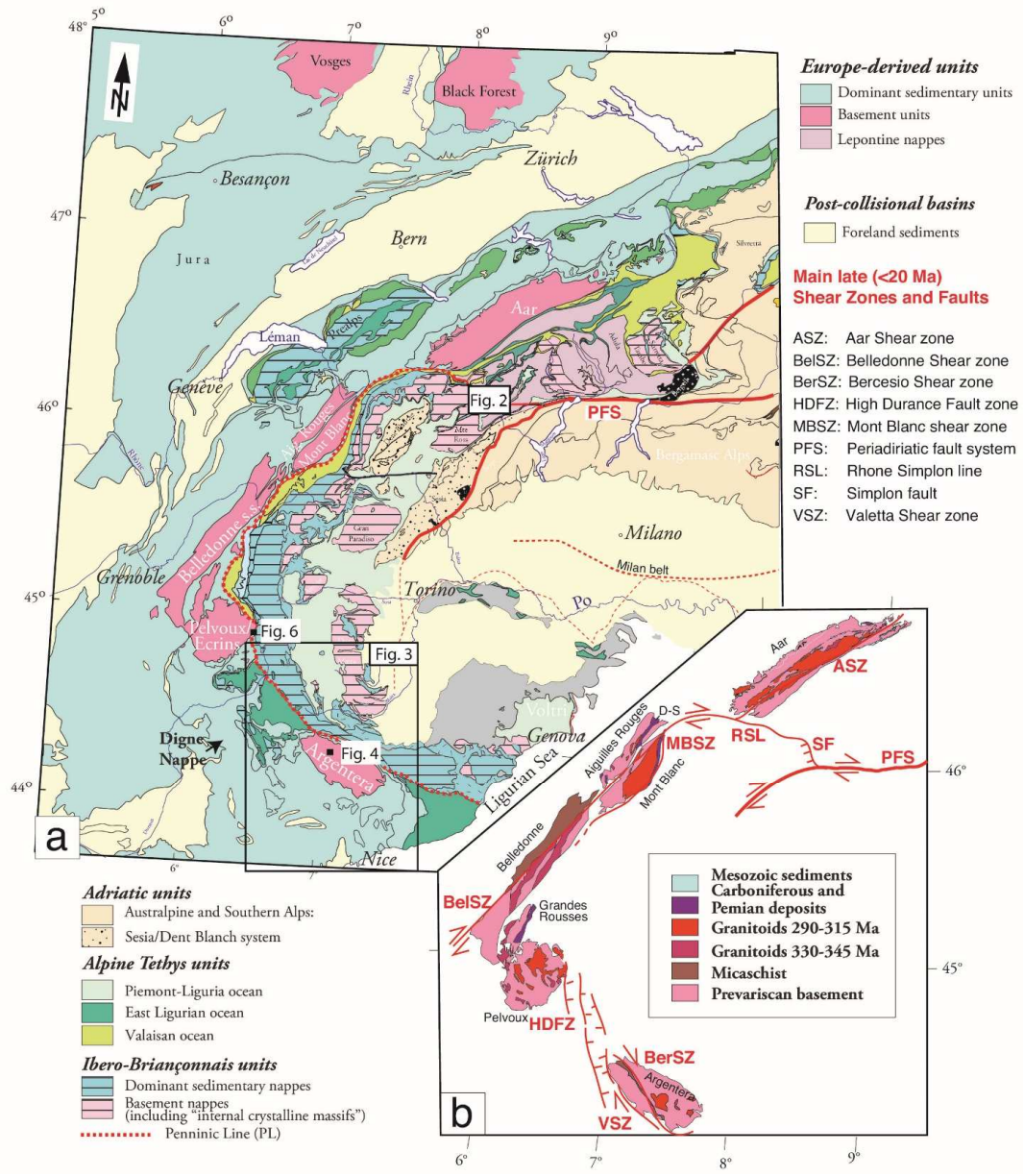

Figure 1. (**a**) Geological map of Western Alps, simplified after [42]. (**b**) Simplified sketch map with the main shear zones and faults reactivating the Penninic Front.

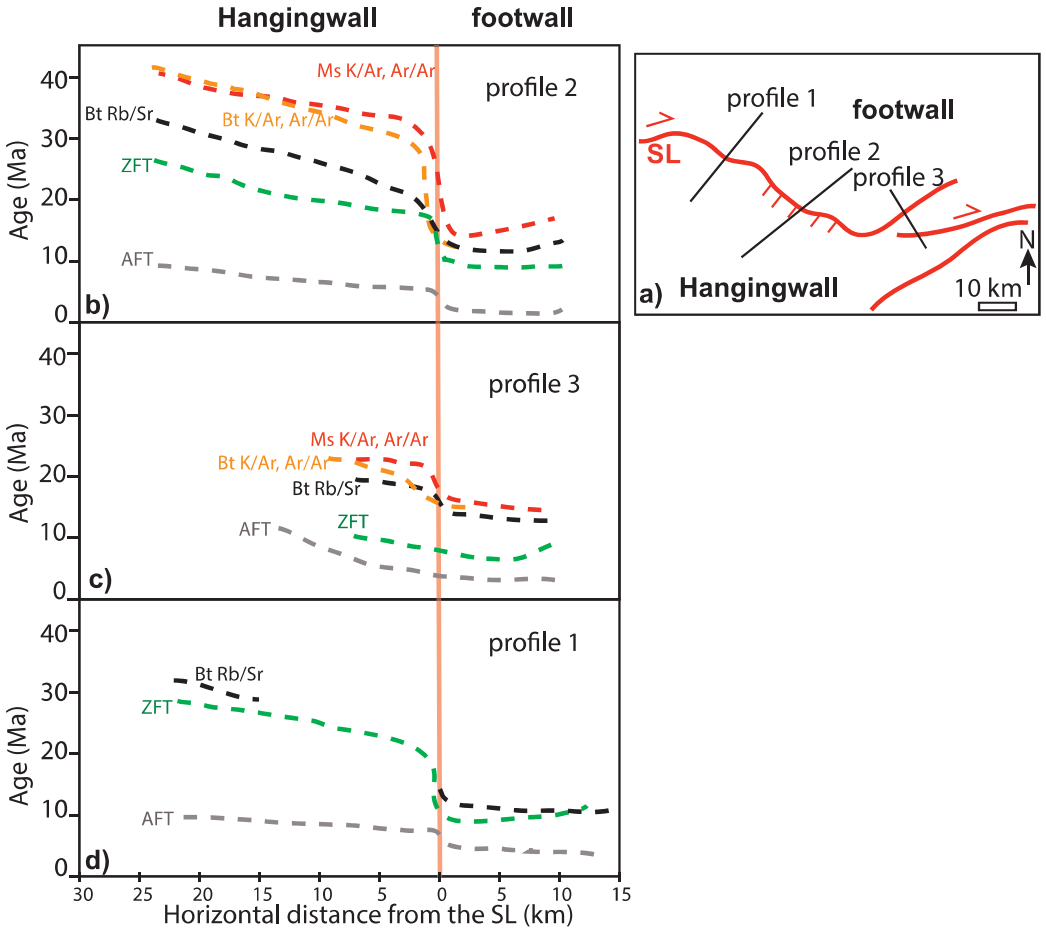

Figure 2. Compilation of a variety of thermochronological ages on both sides of the Simplon normal fault (see location on Figure 1; from [15]). Cooling age patterns across the Simplon Fault Zone. (**a**) Location of three age–distance sections. (**b**) Age–distance section from the central region (central part of Simplon Line or SL. (**c**) Age–distance section from the SE region. (**d**) Age–distance section from the NW region.

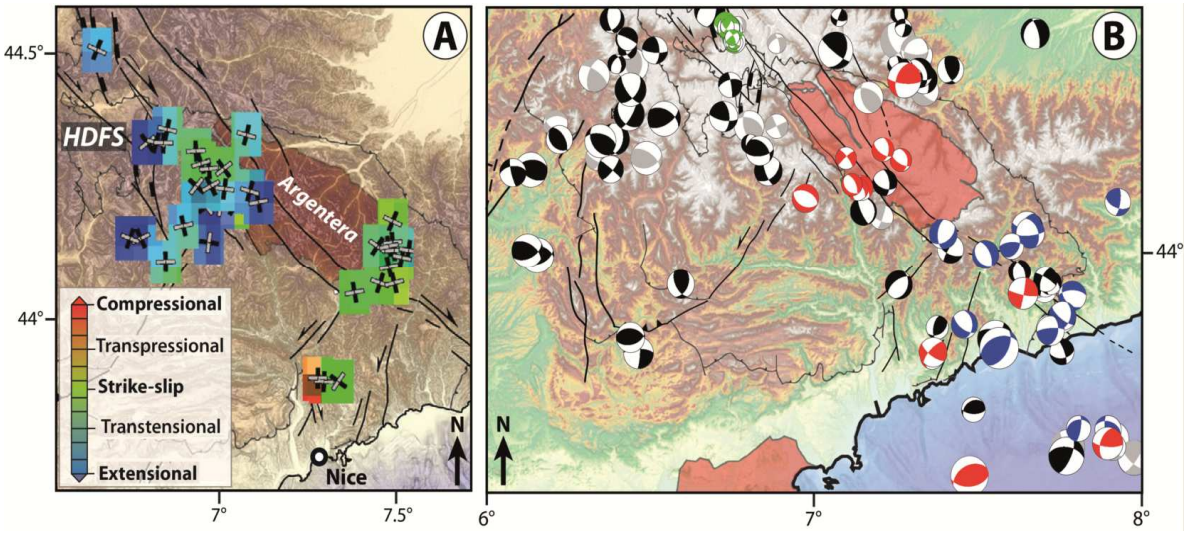

Figure 3. (**A**) Paleostress tensors computed from fault–striae data and (**B**), focal mechanisms of active seismicity from [51]. Note the transition from extension to strike–slip and compression, from NW to SE. HDFS: High Durance Fault System.

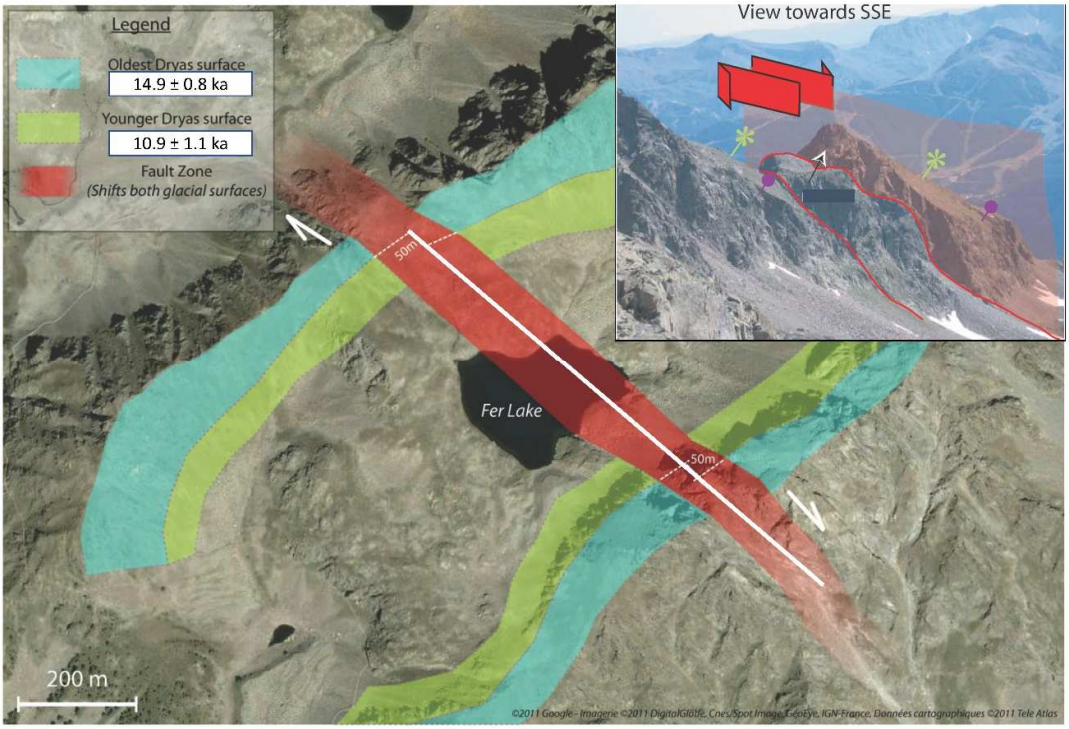

Figure 4. Glacial offset geomorphologies in the Argentera crystalline massif from [27,52]. Polished surfaces were dated with quartz ^{10}Be CRE dating. Green stars in insert landscape photo locate the position of the upper, more gently dipping Oldest Dryas surface, while the purple circles locate the break in slope related to incision of the Younger Dryas.

In the Central Alps, dating of hydrothermal minerals in shear zones surrounding the Lepontine Dome, including parts of the Penninic Line, shows that hydrothermal activity linked to major fault activity has occurred since 19 Ma and was maintained at least until 2.7 Ma [28,30,54,55]. This is also the case in the external crystalline massifs of the NW and W Alps (15–5 Ma; [20], and in the SW Alps (21–15 Ma; [56]; Figure 5). The upper bound of these ages is similar to phyllosilicate crystallization ages [13,15,57,58], which highlights a continuous deformation from ductile to brittle conditions. A similar range of ages is obtained by epidote and monazite U–Pb and phengite Ar/Ar dating along the Penninic Line in the SW Alpine arc (Figure 5, [59]). There, the dextral strike–slip reactivation of the Penninic Line onset is at 26–20 Ma in the Argentera massif [60], whereas U–Pb dating of monazites which crystallized within opened veins in a similar kinematic context returns ages of 21–15 Ma [56]. Based on these data, it is suggested that the Penninic Line has been reactivated as a curved dextral strike–slip fault since about 26 Ma along the whole Alpine arc and has remained in a similar tectonic context until the present (Figure 5, [61–63]). The geologic evidence thus possibly points to an ongoing, though moderate, tectonic activity throughout the Alps over the last 5 Ma. In this time range, and especially after 2 Ma, valley incision has significantly increased in the External Alps, due to the onset of glaciations [64,65]. The lack of syn–kinematic or hydrothermal minerals younger than 2.7 Ma is not proof of cessation of tectonic activity, but a transition to temperatures <200 °C and hence cooling below the crystallization temperature of most datable hydrothermal minerals. The application of thermochronological tools with closure temperatures lower than 70 °C, such as the Apatite He–dating methods, returns ages of 4–5 Ma in the NW part of the Argentera, at the SE boundary of the High Durance Valley extensional system [66], and of 2–5 Ma in the Alpine foreland basin below the Digne Nappe [67]. The question regarding the potential fault activity accompanying this late <5 Ma erosion thus remains open, as no direct fault activity is constrained in this time range. Higher temperature thermochronometers, such as, for

example, zircon fission–track dating, do not show any evidence for increasing erosion or exhumation rates after 5 Ma in the Western Alps [68].

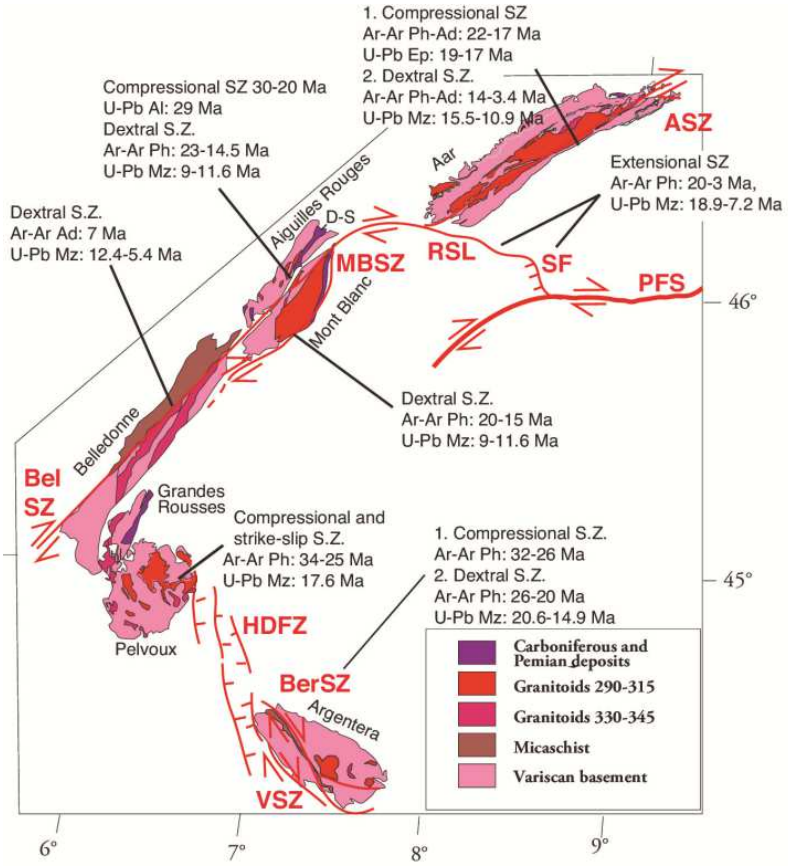

Figure 5. Compilation of Ar–Ar on phengite and U–Pb on allanite/epidote/monazite ages along the Western External Alps. ASZ: Aar Shear zone (Ar–Ar on phengite (Ph) from [57,58], U–Pb on epidote (Ep) by [59] and on monazite (Mz) by [54]); BelSZ: Belledonne Shear Zone (U–Pb on Monazite by [20,23], Ar–Ar on adularia (Ad) by [20]), BerSZ: Bercesio Shear Zone (Ar–Ar on phengite by [60], and U–Pb on monazite by [56]), HDFZ: High Durance Fault System (Ar–Ar on phengite by [14,17], U–Pb on Monazite by [20], MBSZ: Mont Blanc Shear Zone (U–Pb on allanite (Al) by [61] and on Monazite by [62], Ar–Ar on Phengite by [13]); PFS: Periadriadic Fault System, RSL: Rhone Simplon Line and SF: Simplon Fault (Ar–Ar on phengite by [15]; U–Pb on monazite by [63]; VSZ: Valetta Shear Zone (same refs as for BerSZ).

1.2. U–Pb on Calcite Dating of Post–5 Ma Activity along the Penninic Line

The advent of the calcite U–Pb in–situ dating method allows pinpointing of the history of fault activity until about 1 Ma (e.g., [69]). This method allowed dating of a phase of extensional reactivation of the Penninic Line in the High Durance Fault system (HDFS) on the eastern side of the Pelvoux External Crystalline Massif [36]. U–Pb dating was applied to calcite that crystallized in the matrix of a fault zone cataclasite in an extensional fault along the hanging wall of the Penninic Line (Figure 6). Bilau et al. [36] showed that the carbonated cataclasite cement formed during/after the main fault slip event at 3.4 $\pm$ 1.4 Ma. Cross–cutting veins featuring the last fault motions were dated at 2.6 $\pm$ 0.3 and 2.3 $\pm$ 0.2 Ma, which brackets the brittle reactivation of the Penninic Line between c. 4 and 2 Ma, on an east–dipping normal fault likely connected to the Penninic Line, which was reactivated as a detachment. An additional age of 3.5 $\pm$ 0.4 Ma was acquired from a conjugate W–dipping fault set, and a slightly older age (5 Ma) in another normal fault system more to the East (Bilau, [70]). The kinematics of this set of normal faults is in agreement with a dominant down–dip extensional component, which alternates with a minor strike–slip component

between 5 and 2 Ma (as also noted by Sue and Tricart, [37,71,72]). These data show that the extensional reactivation of the HDFS has occured since at least 5 Ma, which suggests a continuous activity over a several Myr period, whereas only the final steps had been documented previously by seismic and GPS data [32]. The surface uplift of the Pelvoux External Crystalline Massif, at a rate of 1 mm·yr^{-1} [73] is fully explained by the relative motion of the footwall ([36], Figure 6f). From this example, it is now clear that tectonic motions have been ongoing over at least the last 5 Ma.

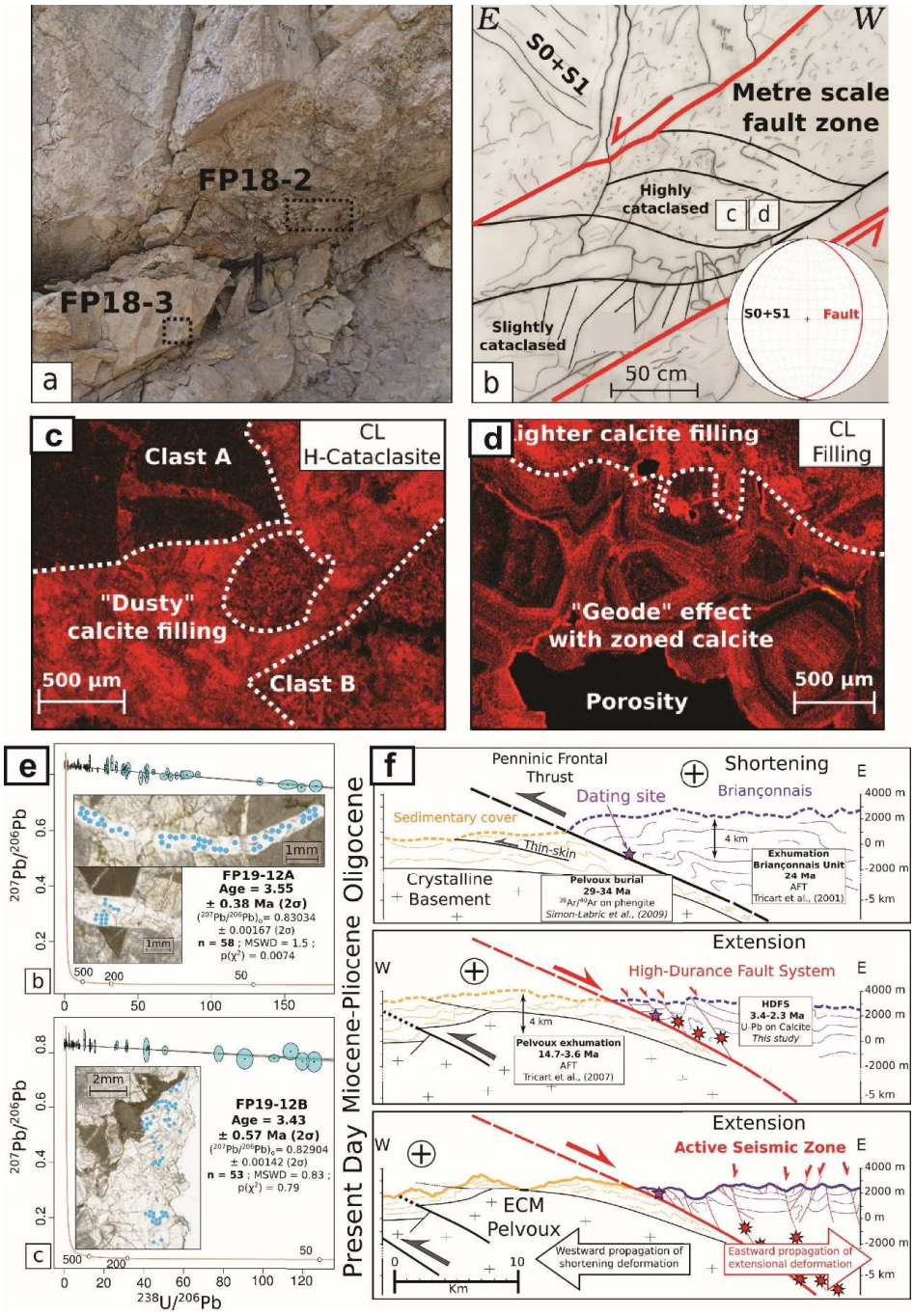

Figure 6. Dated extensional fault in the High Durance Fault System or HDFS [36]. (**a**,**b**) Outcrop relationship of the east–dipping normal fault zone and cataclasite damage zone. (**c**,**d**) Cathodoluminescence images of the dated calcite showing residual porosity within the cataclasite. (**e**) Example of U–Pb results. (**f**) Reconstructed geodynamic scenario of Penninic Line extensional reactivation and formation of the HDFS.

1.3. Western Alpine Foreland Deformation

Independent constraints on tectonic activity in the Alps also come from the peripheral foreland basins, the Molasse basin and the Po Basin (Figure 1), both of which show Quaternary rock uplift, indicating that erosion has recently begun to outpace tectonic crustal thickening leading to flexural isostatic rebound [11,25,74].

1.3.1. Po Depression

At the back of the Alps, deformation is thought to have ceased in the early Pliocene along the Lombardic thrust belt, as suggested by growth strata and thrust–sealing post–tectonic sediments in the Po Basin [75,76]. However, zones with significant subsidence have been measured by GPS in other parts of the Po basin [77] and, in this domain, no field evidence can be used to discuss the vertical motions due to the progressive sediment infill of the basin. Based on seismic profiles [2] and from vertical GPS data [77], it is clear that the Po basin has been subsiding in the last 5 Ma, especially in connection to the Apennine frontal flexural basin. As the Apennines are significantly more active than the Alps, the Alpine subsidence or surface uplift signal in the Po basin remain difficult to disentangle from one another.

1.3.2. Jura Mountains

The frontal fold–and–thrust–belts of the Central Alps apparently ceased a thin–skin tectonic motion in the Pliocene, sometime between 9 and 4 Ma in the Jura Mountains [78] according to analysis of paleontological remains [79] and tectonic evidence. On the basis of a comparison between palaeo–tensors and focal mechanisms, Becker [78] suggested that a new (thick–skin) style of tectonics started after 4 Ma, deforming both the cover rocks and their basement directly in a similar mode. Recently, direct dating of deformation in the eastern Jura fold–and–thrust–belt has allowed bracketing of the thin–skin deformation phase between 14.3 and 4.5 Ma, which suggests that deformation occurred over a time period of at least ~10 Myr, with contemporaneous activity of thrusts and strike–slip faults between 10.5–3.9 Ma [80,81]. Additionally, based on the constant in–situ temperatures and fluid sources reconstructed over the recorded time period, these authors have shown that large–scale foreland erosion initiated after ~4.5 Ma.

Deformation in the Jura Mountains is still active and instrumental seismology shows that strike–slip earthquakes (M < 5.5) occur along NW–SE– to NNW–SSW strike–slip faults with hypocenters at ∼1–5 km depths, both in the sedimentary cover and in the upper part of the crystalline basement [82]. A recent thrust–related earthquake (2004 Besançon earthquake, [83]) had a hypocenter located at ∼15 km depth in the crystalline basement [84]. Geodetic and geological data indicate up to ∼1 mm·yr^{-1} N–S– to NNW–SSE–oriented and ongoing shortening, coupled with ∼0.5 mm·yr^{-1} of surface uplift [78,85–87]. More precisely, surface uplift is located above the main thrusts and anticlines (2004 Besançon thrust–related earthquake located in the crystalline basement; [83]), suggesting both thrust– and fold–related shortening [86,87].

1.3.3. Digne Nappe and SW Alpine Foreland

Thermochronological data coupling fission–track and (U–Th)/He on apatite allow quantification of the sequence of burial and exhumation of Tertiary detrital sediments at the front of the Alpine arc [67]. Parts of the Tertiary basins were buried under the Mesozoic sedimentary cover of the Digne Nappe (Figure 1) and then exhumed. Thermal modelling shows that these basins were covered by 3 to 4 km of sedimentary cover, between 12 and 6 Ma, related to thin–skinned nappe emplacement without major relief development. The onset of exhumation is dated at ~6 Ma and is associated with the formation of a progressively eroded relief (at rates of mm/yr) producing an erosional half–window. This regional exhumation is the consequence of basement involvement in shortening and outward propagation of foreland deformation at 6 Ma.

The SW Alps provides examples of ongoing fault motions from the Paleogene through the Quaternary. In the Provence and Maritime Alps foreland, Quaternary activity of faults is evidenced by several authors (e. g., [29,31,51,88] and refs therein). These faults are sub–vertical and are mostly strike–slip faults with a thrust component. They may be influenced by the presence of salt at depth in the Triassic horizons [30]. However, due to their very slow relative motions (0.02–0.3 mm·yr^{-1}; [31,89–91]), which are slower or comparable to denudation rates (about 0.030–0.1 mm·yr^{-1}, [89,91–93]), the geomorphological markers of these recent fault motions are generally not preserved. Similar stress paleo–tensors are obtained with fault–striae data inversions and focal mechanism analysis, thus suggesting a continuity of long–term brittle deformation (<15 Ma) with the active deformation ([51]; Figure 3).

2. Origin of the Alpine Relief: The Imprint of Repeated Glacial Cycles

Possibly increasing erosion since 5 Ma, especially focused in main valleys since 2 Ma, leads to further questions about the relative roles of climate change and tectonics, as this date coincides with the onset of glacial cycles [24,25,74,94]). The contribution of several parameters to uplift rate has been modelled by Sternai et al. [95] and these authors suggest that the contribution of deglaciation is about 50%, whereas the other 50% is associated with deep processes (slab retreat or convection cell) in the Western and Central Alps. Increased erosion in the external crystalline massifs has been documented by numerous authors, to the north and west of the Penninic Line (e.g., [96] and references therein). However, thermo–kinematic modelling, including a temporally evolving topography, suggests a steady state, long–term exhumation [97] and recent data highlight a relatively constant exhumation [9]. Therefore, this last 5–Ma phase is mainly expressed by localized valley incision, as demonstrated by apatite helium and $^{4}He/^{3}He$ studies [64], implying a significant increase in local relief through valley incision. As stressed by [12], this focused erosion might lead to overestimation of erosion rates on a more regional scale.

3. Uplift after the Würm Glaciation: The Constraints Provided by Cosmogenic Nuclide Dating of Incision

The incision pattern of rivers in the SW Alps has recently been constrained through CRE dating by several studies [98–104] (Figure 7). The lower bound of compiled incision data from the whole SW Alps gives a similar range of values to those provided by GPS measurements (<0.5 mm·yr^{-1}; [26,34]), suggesting that geodetic estimates give comparable surface uplift rate values to those running through an interglacial (Holocene) cycle. In the SW Alps, two domains of different incision regimes are shown by the CRE dating of gorge walls polished by rivers [104]. In the upstream part of rivers, in valleys under glacial influence, the incision rates are more variable and can be significantly higher, suggesting a topographic readjustment by the rivers [99]. This pattern is in agreement with the preservation of a stepped river profile, inherited from several glacial phases and which cannot be totally smoothed during interglacial phases [99,105]. This goes with the suggestion that, during interglacials, incision of formerly glaciated catchments largely exceeds the regional surface uplift signal. Conversely, in low–elevation valley catchments out of the domain of influence of glaciers, incision rates of rivers seem to have reached equilibrium. In these domains out of the influence of glaciers, river incision rates (~0.05 mm/yr) are similar to the erosion rates estimated by cosmogenic analyses of the bulk sediment signal [102,106] and have values similar to the regional uplift rate in agreement with GPS measures (Figure 7), suggesting a steady state between erosion and surface uplift.

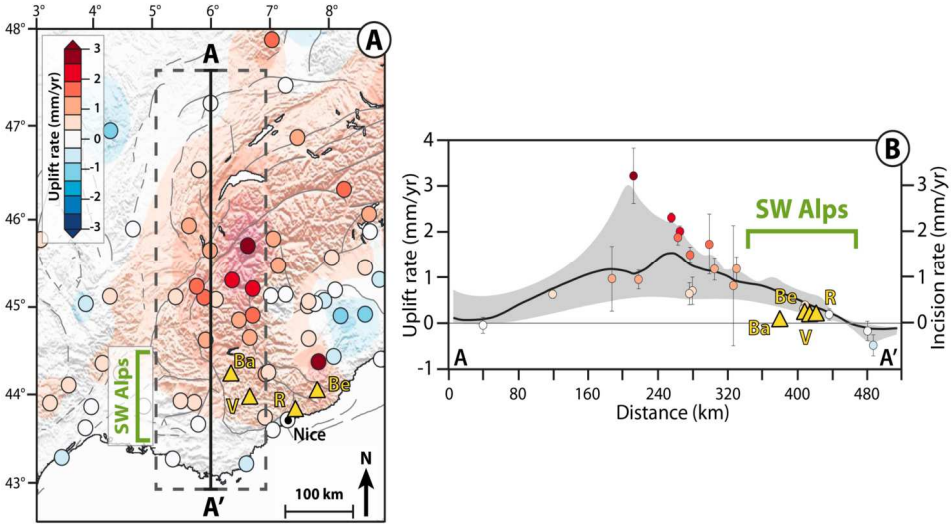

Figure 7. Long–term incision pattern of rivers of the SW Alps, out of the zone affected by glacial influence, constrained by CRE dating (data from [98–104]). (**A**), Vertical velocity field (colored circles) map of the Western Alps made by [77], with the location of gorges dated with ^{36}Cl cosmonuclide dating (yellow triangles): Ba, Barles [103]; V, Verdon, R, Rédébraus, Be, Bendola (Cardinal et al., in review). Positive (red) and negative (blue) values represent surface uplift or subsidence, respectively. (**B**) Vertical uplift estimated by GPS [77] and incision rates estimated from ^{36}Cl cosmonuclide dating versus distance. The black curve shows the median value of the vertical uplift rate, whereas the grey envelope shows the minimum and maximum vertical uplift rate values in the swath. Estimated incision rates have similar mean values to that of GPS rates, in the SW Alps.

4. Conclusions: 'Bridging the Gap' between the Long–Term (>10 Ma Scale) and Current Evolution of Orogens

Based on the combined dating approaches of thermochronology, and direct dating of fault motions and geomorphological features in the Alps, we conclude in this paper that it becomes possible to decipher the evolution of a mountain belt from the geological past to recent times (<1 Ma). To infer the activity of faults in the long term, it is necessary to obtain direct dating of fault slip. In the Alps, calcite U–Pb dating allowed the pinpointing the fault activity on a scale of <3 Ma. The data show the development of the foreland basins until 5 Ma, and the onset of their widespread erosion. The 5 Ma transition is highlighted by the activity of mainly extensional motions along the Penninic Line in the High Durance valley, with paleo–tensors from fault-striae inversion similar to the present–day focal mechanisms. Along the whole Alpine arc, and especially in the foreland part, the currently monitored seismicity is mainly in agreement with slow transcurrent and compressional kinematics. Faults are mainly right–lateral along or slightly oblique to the belt strike. Therefore, the post–5–Ma period is neither a period of complete shift towards generalized extension, nor a period of cessation of tectonic activity, but, more likely, a period of slowing down of tectonic motions. At a larger scale, the tectonics are in agreement with an anticlockwise rotation of the Apulian Plate, which is also related to Apulian slab roll–back and back–arc basin opening of the Ligurian and Tyrrhenian basins (Figure 8). This regional phenomenon could also be apparent from the SKS splitting measurements pattern at mantle depths [107], suggestive of the mantle flow beneath the Alps. It may be that the slowing down of tectonic motions, and of the corresponding Apulian rotations at 5 Ma, could be related to the decrease in the roll–back process. The slowing down of Apulian rotation is, however, accompanied by a trend towards a cooler climate, which has favored a regained erosion process in the inner part of the belt. The role of efficient glacial erosion and of post–glacial isostatic uplift combined to focused river incision likely played a major role in shaping the mountain belt. However, this process is clearly very heterogeneous spatially, and has been especially focused in the major Alpine valleys, so it led to an amplification of the Alpine

relief and to the deepening of valleys rather than to a generalized and smoothed erosional pattern.

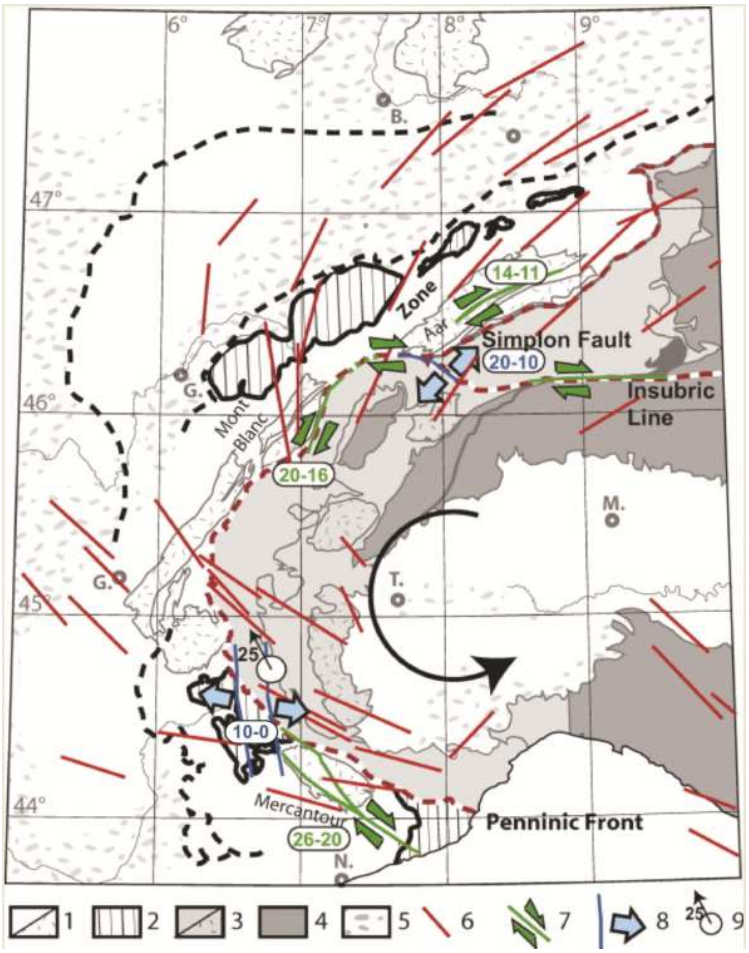

Figure 8. Post–collisional crustal and upper–mantle strain field of the Western Alps with polarities and ages of ductile crustal deformation, and direction of upper–mantle deformation inferred from seismic anisotropies [107]. Age and polarities of displacements are from [58] in the Aar Massif, from [15] in the Simplon Fault Zone, from [13] in the Mont Blanc, and from [60] in the Mercantour. The legend displays: 1, the Dauphinois (or Helvetic) zone, rimmed by the Jura and Alpine frontal thrusts. The Dauphinois zone is comprised of Hercynian crystalline basement (stripped) and its para–autochthonous and allochtonous Mesozoic sedimentary cover (white); 2, the transported klippe of the Helminthoid Upper Cretaceous flysch and Internal Briançonnais and Penninic units. The Internal Alps comprise: 3, the Briançonnais and Piemontais zones, which are made of variably metamorphosed rocks from the continental European margin and the Alpine Tethys oceanic domain; 4, the Austro–Alpine units comprising the Dent Blanche klippe and the Apulian margin; 5, Molasse sediments deposited during the Oligocene to Pliocene lie in the periphery of the Alps. 6, Upper mantle anisotropy defined from systematic SKS splitting measurements [107]. 7 and 8, Main ductile to brittle post–collisional shear zones: 7, strike–slip shear zones; 8 extensional shear zones. 9, Paleomagnetic data obtained in the Briançonnais Zone of SW Alps indicate minimum ∼25° counterclockwise rotation [39]. Ductile mid–crustal deformation is evidenced by mylonites formed in a right–lateral kinematic setting along the Alpine arc. These motions are dated at 26–20 Ma in the South [60], at 20–16 Ma in the West (Mont Blanc; [13]) and 20–12 Ma in the North (Aar; [57,58]). This ductile deformation is suggested to continue in the brittle domain, as shown by similar kinematics of faults dated by calcite U/Pb [36] and AFT between 10 and 0 Ma in the southwest part of the arc (Figure 6). Similar kinematics are shown by fault offset of geomorphological features dated by ^{10}Be on quartz (Figure 4) and seismicity (Figure 3).

Author Contributions: Y.R. wrote the synthesis based on A.B., T.C., D.B., A.N. and L.B. results, with their feedback on the manuscript writing. S.S. and M.B. participated in discussions and final manuscript check. All authors have read and agreed to the published version of the manuscript.

Funding: This research was funded by BRGM-RGF Alps grant. The APC was funded by invitation of Geosciences Journal.

Acknowledgments: This work is based on the masters and Ph.D. results from A. Bilau (U–Pb dating of calcite) and T. Cardinal (river geomorphology) funded by the BRGM in the frame of the RGF–Alps project, on the master thesis of D. Bienveignant (tectonics and U–Pb dating of calcite) and internship of L. Boschetti (structural geology), supported by Edytem and ISTerre laboratories. This manuscript benefited from constructive and positive reviews from two anonymous reviewers and efficient handling by the editorial team.

Conflicts of Interest: The authors declare no conflict of interest.

References

1. Vernant, P.; Hivert, F.; Chery, J.; Steer, P.; Cattin, R.; Rigo, A. Erosion–Induced Isostatic Rebound Triggers Extension in Low Convergent Mountain Ranges. *Geology* **2013**, *41*, 467–470. [CrossRef]
2. Nouibat, A.; Stehly, L.; Paul, A.; Schwartz, S.; Bodin, T.; Dumont, T.; Rolland, Y.; Brossier, R.; Team, C.; Group, A.W. Lithospheric Transdimensional Ambient–Noise Tomography of W–Europe: Implications for Crustal–Scale Geometry of the W–Alps. *Geophys. J. Int.* **2022**, *229*, 862–879. [CrossRef]
3. Mathey, M.; Sue, C.; Pagani, C.; Baize, S.; Walpersdorf, A.; Bodin, T.; Husson, L.; Hannouz, E.; Potin, B. Present–Day Geodynamics of the Western Alps: New Insights from Earthquake Mechanisms. *Solid Earth* **2021**, *12*, 1661–1681. [CrossRef]
4. Schwartz, S.; Lardeaux, J.M.; Tricart, P.; Guillot, S.; Labrin, E. Diachronous exhumation of HP–LT rocks from southwestern Alps: Evidence from fission–track analysis. *Terra Nova* **2007**, *19*, 133–140. [CrossRef]
5. Tricart, P.; Van Der Beek, P.; Schwartz, S.; Labrin, E. Diachronous Late–Stage Exhumation across the Western Alpine Arc: Constraints from Apatite Fission–Track Thermochronology between the Pelvoux and Dora–Maira Massifs. *J. Geol. Soc.* **2007**, *164*, 163–174. [CrossRef]
6. Beucher, R.; van der Beek, P.; Braun, J.; Batt, G.E. Exhumation and Relief Development in the Pelvoux and Dora–Maira Massifs (Western Alps) Assessed by Spectral Analysis and Inversion of Thermochronological Age Transects. *J. Geophys. Res. Earth Surf.* **2012**, *117*. [CrossRef]
7. Glotzbach, C.; Reinecker, J.; Danišík, M.; Rahn, M.; Frisch, W.; Spiegel, C. Thermal History of the Central Gotthard and Aar Massifs, European Alps: Evidence for Steady State, Long–Term Exhumation. *J. Geophys. Res. Earth Surf.* **2010**, *115*. [CrossRef]
8. Reinecker, J.; Danišík, M.; Schmid, C.; Glotzbach, C.; Rahn, M.; Frisch, W.; Spiegel, C. Tectonic Control on the Late Stage Exhumation of the Aar Massif (Switzerland): Constraints from Apatite Fission Track and (U–Th)/He Data. *Tectonics* **2008**, *27*. [CrossRef]
9. Girault, J.B.; Bellahsen, N.; Bernet, M.; Pik, R.; Loget, N.; Lasseur, E.; Rosenberg, C.L.; Balvay, M.; Sonnet, M. Exhumation of the Western Alpine Collisional Wedge: New Thermochronological Data. *Tectonophysics* **2022**, *822*, 229155. [CrossRef]
10. Schildgen, T.F.; van der Beek, P.A.; Sinclair, H.D.; Thiede, R.C. Spatial Correlation Bias in Late–Cenozoic Erosion Histories Derived from Thermochronology. *Nature* **2018**, *559*, 89–93. [CrossRef]
11. Willett, S.D.; Herman, F.; Fox, M.; Stalder, N.; Ehlers, T.A.; Jiao, R.; Yang, R. Bias and Error in Modelling Thermochronometric Data: Resolving a Potential Increase in Plio–Pleistocene Erosion Rate. *Earth Surf. Dyn.* **2021**, *9*, 1153–1221. [CrossRef]
12. Van der Beek, P.; Schildgen, T.; Thiede, R.; Sinclair, H. Bias and error in modelling thermochronology data: A comment on Willett et al. *Earth Surf. Dynam. Dis.* **2020**, *9*, 1153–1221. [CrossRef]
13. Rolland, Y.; Rossi, M.; Cox, S.; Corsini, M.; Mancktelow, N.; Pennacchioni, G.; Fornari, M.; Boullier, A.-M. 40Ar/39Ar Dating of Synkinematic White Mica: Insights from Fluid–Rock Reaction in Low–Grade Shear Zones (Mont Blanc Massif) and Constraints on Timing of Deformation in the NW External Alps. *Geol. Soc. Lond. Spec. Publ.* **2008**, *299*, 293–315. [CrossRef]
14. Simon-Labric, T.; Rolland, Y.; Dumont, T.; Heymes, T.; Authemayou, C.; Corsini, M.; Fornari, M. 40Ar/39Ar Dating of Penninic Front Tectonic Displacement (W Alps) during the Lower Oligocene (31–34 Ma). *Terra Nova* **2009**, *21*, 127–136. [CrossRef]
15. Campani, M.; Mancktelow, N.; Seward, D.; Rolland, Y.; Müller, W.; Guerra, I. Geochronological Evidence for Continuous Exhumation through the Ductile–Brittle Transition along a Crustal–Scale Low–Angle Normal Fault: Simplon Fault Zone, Central Alps. *Tectonics* **2010**, *29*. [CrossRef]
16. Wiederkehr, M.; Sudo, M.; Bousquet, R.; Berger, A.; Schmid, S.M. Alpine Orogenic Evolution from Subduction to Collisional Thermal Overprint: The 40Ar/39Ar Age Constraints from the Valaisan Ocean, Central Alps. *Tectonics* **2009**, *28*. [CrossRef]
17. Bellanger, M.; Augier, R.; Bellahsen, N.; Jolivet, L.; Monié, P.; Baudin, T.; Beyssac, O. Shortening of the European Dauphinois Margin (Oisans Massif, Western Alps): New Insights from RSCM Maximum Temperature Estimates and 40Ar/39Ar in Situ Dating. *J. Geodyn.* **2015**, *83*, 37–64. [CrossRef]

18. Bergemann, C.; Gnos, E.; Berger, A.; Whitehouse, M.; Mullis, J.; Wehrens, P.; Pettke, T.; Janots, E. Th–Pb Ion Probe Dating of Zoned Hydrothermal Monazite and Its Implications for Repeated Shear Zone Activity: An Example from the Central Alps, Switzerland. *Tectonics* **2017**, *36*, 671–689. [CrossRef]
19. Berger, A.; Gnos, E.; Janots, E.; Whitehouse, M.; Soom, M.; Frei, R.; Waight, T.E. Dating Brittle Tectonic Movements with Cleft Monazite: Fluid–Rock Interaction and Formation of REE Minerals. *Tectonics* **2013**, *32*, 1176–1189. [CrossRef]
20. Gasquet, D.; Bertrand, J.-M.; Paquette, J.-L.; Lehmann, J.; Ratzov, G.; de Ascencao Guedes, R.; Tiepolo, M.; Boullier, A.-M.; Scaillet, S.; Nomade, S. Miocene to Messinian Deformation and Hydrothermal Activity in a Pre–Alpine Basement Massif of the French Western Alps: New U–Th–Pb and Argon Ages from the Lauzière Massif. *Bull. Soc. Géolog. Fr.* **2010**, *181*, 227–241. [CrossRef]
21. Gnos, E.; Janots, E.; Berger, A.; Whitehouse, M.; Walter, F.; Pettke, T.; Bergemann, C. Age of Cleft Monazites in the Eastern Tauern Window: Constraints on Crystallization Conditions of Hydrothermal Monazite. *Swiss J. Geosci.* **2015**, *108*, 55–74. [CrossRef]
22. Grand'Homme, A.; Janots, E.; Seydoux-Guillaume, A.-M.; Guillaume, D.; Bosse, V.; Magnin, V. Partial Resetting of the U–Th–Pb Systems in Experimentally Altered Monazite: Nanoscale Evidence of Incomplete Replacement. *Geology* **2016**, *44*, 431–434. [CrossRef]
23. Janots, E.; Grand'Homme, A.; Bernet, M.; Guillaume, D.; Gnos, E.; Boiron, M.-C.; Rossi, M.; Seydoux-Guillaume, A.-M.; De Ascenção Guedes, R. Geochronological and Thermometric Evidence of Unusually Hot Fluids in an Alpine Fissure of Lauzière Granite (Belledonne, Western Alps). *Solid Earth* **2019**, *10*, 211–223. [CrossRef]
24. Herman, F.; Seward, D.; Valla, P.G.; Carter, A.; Kohn, B.; Willett, S.D.; Ehlers, T.A. Worldwide Acceleration of Mountain Erosion under a Cooling Climate. *Nature* **2013**, *504*, 423–426. [CrossRef] [PubMed]
25. Champagnac, J.D.; Molnar, P.; Anderson, R.S.; Sue, C.; Delacou, B. Quaternary Erosion–Induced Isostatic Rebound in the Western Alps. *Geology* **2007**, *35*, 195–198. [CrossRef]
26. Nocquet, J. –M.; Sue, C.; Walpersdorf, A.; Tran, T.; Lenôtre, N.; Vernant, P.; Cushing, M.; Jouanne, F.; Masson, F.; Baize, S.; et al. Present–Day Uplift of the Western Alps. *Sci. Rep.* **2016**, *6*, 28404. [CrossRef]
27. Sanchez, G.; Rolland, Y.; Corsini, M.; Braucher, R.; Bourlès, D.; Arnold, M.; Aumaître, G. Relationships between Tectonics, Slope Instability and Climate Change: Cosmic Ray Exposure Dating of Active Faults, Landslides and Glacial Surfaces in the SW Alps. *Geomorphology* **2010**, *117*, 1–13. [CrossRef]
28. Sanchez, G.; Rolland, Y.; Schreiber, D.; Giannerini, G.; Corsini, M.; Lardeaux, J.-M. The Active Fault System of SW Alps. *J. Geodyn.* **2010**, *49*, 296–302. [CrossRef]
29. Jomard, H.; Cushing, E.M.; Palumbo, L.; Baize, S.; David, C.; Chartier, T. Transposing an Active Fault Database into a Seismic Hazard Fault Model for Nuclear Facilities–Part 1: Building a Database of Potentially Active Faults (BDFA) for Metropolitan France. *Nat. Hazards Earth Syst. Sci.* **2017**, *17*, 1573–1584. [CrossRef]
30. Bauve, V.; Rolland, Y.; Sanchez, G.; Giannerini, G.; Schreiber, D.; Corsini, M.; Perez, J.-L.; Romagny, A. Pliocene to Quaternary Deformation in the Var Basin (Nice, SE France) and Its Interpretation in Terms of "Slow–Active" Faulting. *Swiss J. Geosci.* **2012**, *105*, 361–376. [CrossRef]
31. Thomas, F.; Rizza, M.; Bellier, O.; Billant, J.; Dussouillez, P.; Fleury, J.; Delanghe, D.; Ollivier, V.; Godard, V.; Talon, B. Assessing Post–Pliocene Deformation in a Context of Slow Tectonic Deformation: Insights from Paleoseismology, Remote Sensing and Shallow Geophysics in Provence, France. *Nat. Hazards* **2021**, *105*, 1453–1490. [CrossRef]
32. Walpersdorf, A.; Pinget, L.; Vernant, P.; Sue, C.; Deprez, A.; The RENAG team. Does Long–Term GPS in the Western Alps Finally Confirm Earthquake Mechanisms? *Tectonics* **2018**, *37*, 3721–3737. [CrossRef]
33. Mathey, M.; Walpersdorf, A.; Sue, C.; Baize, S.; Deprez, A. Seismogenic Potential of the High Durance Fault Constrained by 20 Yr of GNSS Measurements in the Western European Alps. *Geophys. J. Int.* **2020**, *222*, 2136–2146. [CrossRef]
34. Piña-Valdés, J.; Socquet, A.; Beauval, C.; Doin, M.-P.; D'Agostino, N.; Shen, Z.-K. 3D GNSS Velocity Field Sheds Light on the Deformation Mechanisms in Europe: Effects of the Vertical Crustal Motion on the Distribution of Seismicity. *J. Geophys. Res. Solid Earth* **2022**, *127*, e2021JB023451. [CrossRef]
35. Tricart, P.; Schwartz, S.; Sue, C.; Poupeau, G.; Lardeaux, J.M. The tectonic denudation of the Ultradauphiné Zone and the inversion of the Briançonnais frontal thrust to the southeast of the Pelvoux massif (western Alps): A Miocene to present–day dynamics. *Bull. Soc. Géol. Fr.* **2001**, *1*, 49–58. [CrossRef]
36. Bilau, A.; Rolland, Y.; Schwartz, S.; Godeau, N.; Guihou, A.; Deschamps, P.; Brigaud, B.; Noret, A.; Dumont, T.; Gautheron, C. Extensional Reactivation of the Penninic Frontal Thrust 3 Myr Ago as Evidenced by U–Pb Dating on Calcite in Fault Zone Cataclasite. *Solid Earth* **2021**, *12*, 237–251. [CrossRef]
37. Sue, C.; Tricart, P. Late Alpine Brittle Extension above the Frontal Pennine Thrust near Briançon, Western Alps. *Eclogae Geol. Helv.* **1999**, *92*, 171–181.
38. Delacou, B.; Sue, C.; Champagnac, J.-D.; Burkhard, M. Present–Day Geodynamics in the Bend of the Western and Central Alps as Constrained by Earthquake Analysis. *Geophys. J. Int.* **2004**, *158*, 753–774. [CrossRef]
39. Collombet, M.; Thomas, J.C.; Chauvin, A.; Tricart, P.; Bouillin, J.P.; Gratier, J.P. Counterclockwise Rotation of the Western Alps since the Oligocene: New Insights from Paleomagnetic Data. *Tectonics* **2002**, *21*, 11–15. [CrossRef]
40. Rolland, Y.; Lardeaux, J.-M.; Jolivet, L. Deciphering Orogenic Evolution. *J. Geodyn.* **2012**, *56*, 1–6. [CrossRef]
41. Bertrand, A.; Sue, C. Reconciling Late Faulting over the Whole Alpine Belt: From Structural Analysis to Geochronological Constrains. *Swiss J. Geosci.* **2017**, *110*, 565–580. [CrossRef]

42. Herwegh, M.; Berger, A.; Bellahsen, N.; Rolland, Y.; Kissling, E. Evolution of the External Crystalline Massifs of the European Alps: From Massif to Lithosphere Scale. *ISTE Ed.* **2022**, *in press*.
43. Jenatton, L.; Guiguet, R.; Thouvenot, F.; Daix, N. The 16,000–Event 2003–2004 Earthquake Swarm in Ubaye (French Alps). *J. Geophys. Res. Solid Earth* **2007**, *112*. [CrossRef]
44. Sue, C.; Thouvenot, F.; Fréchet, J.; Tricart, P. Widespread Extension in the Core of the Western Alps Revealed by Earthquake Analysis. *J. Geophys. Res.Solid Earth* **1999**, *104*, 25611–25622. [CrossRef]
45. Seward, D.; Mancktelow, N.S. Neogene Kinematics of the Central and Western Alps: Evidence from Fission–Track Dating. *Geology* **1994**, *22*, 803–806. [CrossRef]
46. Malusà, M.G.; Polino, R.; Zattin, M.; Bigazzi, G.; Martin, S.; Piana, F. Miocene to Present Differential Exhumation in the Western Alps: Insights from Fission Track Thermochronology. *Tectonics* **2005**, *24*. [CrossRef]
47. Fox, M.; Herman, F.; Kissling, E.; Willett, S.D. Rapid Exhumation in the Western Alps Driven by Slab Detachment and Glacial Erosion. *Geology* **2015**, *43*, 379–382. [CrossRef]
48. Fox, M.; Herman, F.; Willett, S.D.; Schmid, S.M. The Exhumation History of the European Alps Inferred from Linear Inversion of Thermochronometric Data. *Am. J. Sci.* **2016**, *316*, 505–541. [CrossRef]
49. Persaud, M.; Pfiffner, O.-A. Active Deformation in the Eastern Swiss Alps: Post–Glacial Faults, Seismicity and Surface Uplift. *Tectonophysics* **2004**, *385*, 59–84. [CrossRef]
50. Egli, D.; Mancktelow, N. The Structural History of the Mont Blanc Massif with Regard to Models for Its Recent Exhumation. *Swiss J. Geosci.* **2013**, *106*, 469–489. [CrossRef]
51. Bauve, V.; Plateaux, R.; Rolland, Y.; Sanchez, G.; Bethoux, N.; Delouis, B.; Darnault, R. Long–Lasting Transcurrent Tectonics in SW Alps Evidenced by Neogene to Present–Day Stress Fields. *Tectonophysics* **2014**, *621*, 85–100. [CrossRef]
52. Darnault, R.; Rolland, Y.; Braucher, R.; Bourlès, D.; Revel, M.; Sanchez, G.; Bouissou, S. Timing of the Last Deglaciation Revealed by Receding Glaciers at the Alpine–Scale: Impact on Mountain Geomorphology. *Quat. Sci. Rev.* **2012**, *31*, 127–142. [CrossRef]
53. Leclère, H.; Cappa, F.; Faulkner, D.; Fabbri, O.; Armitage, P.; Blake, O. Development and Maintenance of Fluid Overpressures in Crustal Fault Zones by Elastic Compaction and Implications for Earthquake Swarms. *J. Geophys. Res. Solid Earth* **2015**, *120*, 4450–4473. [CrossRef]
54. Ricchi, E.; Bergemann, C.; Gnos, E.; Berger, A.; Rubatto, D.; Whitehouse, M. Constraining Deformation Phases in the Aar Massif and the Gotthard Nappe (Switzerland) Using Th–Pb Crystallization Ages of Fissure Monazite–(Ce). *Lithos* **2019**, *342*, 223–238. [CrossRef]
55. Bergemann, C.A.; Gnos, E.; Berger, A.; Janots, E.; Whitehouse, M.J. Dating Tectonic Activity in the Lepontine Dome and Rhone–Simplon Fault Regions through Hydrothermal Monazite–(Ce). *Solid Earth* **2020**, *11*, 199–222. [CrossRef]
56. Ricchi, E.; Gnos, E.; Rubatto, D.; Whitehouse, M.J.; Pettke, T. Ion Microprobe Dating of Fissure Monazite in the Western Alps: Insights from the Argentera Massif and the Piemontais and Briançonnais Zones. *Swiss J. Geosci.* **2020**, *113*, 15. [CrossRef]
57. Challandes, N.; Marquer, D.; Villa, I.M. PTt Modelling, Fluid Circulation, and 39Ar–40Ar and Rb–Sr Mica Ages in the Aar Massif Shear Zones (Swiss Alps). *Swiss J. Geosci.* **2008**, *101*, 269–288. [CrossRef]
58. Rolland, Y.; Cox, S.F.; Corsini, M. Constraining Deformation Stages in Brittle–Ductile Shear Zones from Combined Field Mapping and 40Ar/39Ar Dating: The Structural Evolution of the Grimsel Pass Area (Aar Massif, Swiss Alps). *J. Struct. Geol.* **2009**, *31*, 1377–1394. [CrossRef]
59. Peverelli, V.; Ewing, T.; Rubatto, D.; Wille, M.; Berger, A.; Villa, I.M.; Lanari, P.; Pettke, T.; Herwegh, M. U– Pb Geochronology of Epidote by Laser Ablation Inductively Coupled Plasma Mass Spectrometry (LA–ICP–MS) as a Tool for Dating Hydrothermal–Vein Formation. *Geochronology* **2021**, *3*, 123–147. [CrossRef]
60. Sanchez, G.; Rolland, Y.; Schneider, J.; Corsini, M.; Oliot, E.; Goncalves, P.; Verati, C.; Lardeaux, J.-M.; Marquer, D. Dating Low–Temperature Deformation by 40Ar/39Ar on White Mica, Insights from the Argentera–Mercantour Massif (SW Alps). *Lithos* **2011**, *125*, 521–536. [CrossRef]
61. Cenki-Tok, B.; Darling, J.R.; Rolland, Y.; Dhuime, B.; Storey, C.D. Direct dating of mid-crustal shear zones with synkinematic allanite: New in situ U-Th-Pb geochronological approaches applied to the Mont Blanc massif. *Terra Nova* **2014**, *26*, 29–37. [CrossRef]
62. Bergemann, C.A.; Gnos, E.; Whitehouse, M.J. Insights into the tectonic history of the Western Alps through dating of fissure monazite in the Mont Blanc and Aiguilles Rouges Massifs. *Tectonophysics* **2019**, *750*, 203–212. [CrossRef]
63. Gnos, E.; Mullis, J.; Ricchi, E.; Bergemann, C.A.; Janots, E.; Berger, A. Episodes of Fissure Formation in the Alps: Connecting Quartz Fluid Inclusion, Fissure Monazite Age, and Fissure Orientation Data. *Swiss J. Geosci.* **2021**, *114*, 14. [CrossRef] [PubMed]
64. Valla, P.G.; Shuster, D.L.; Van Der Beek, P.A. Significant Increase in Relief of the European Alps during Mid–Pleistocene Glaciations. *Nat. Geosci.* **2011**, *4*, 688–692. [CrossRef]
65. Nibourel, L.; Rahn, M.; Dunkl, I.; Berger, A.; Herman, F.; Diehl, T.; Heuberger, M. Orogen-Parallel Migration of Exhumation in the Eastern Aar Massif Revealed by Low-T Thermochronometry. *J. Geophys. Res. Solid Earth* **2021**, *126*, e2020JB020799. [CrossRef]
66. Sanchez, G.; Rolland, Y.; Jolivet, M.; Brichau, S.; Corsini, M.; Carter, A. Exhumation Controlled by Transcurrent Tectonics: The Argentera–Mercantour Massif (SW Alps). *Terra Nova* **2011**, *23*, 116–126. [CrossRef]
67. Schwartz, S.; Gautheron, C.; Audin, L.; Dumont, T.; Nomade, J.; Barbarand, J.; Pinna–Jamme, R.; van der Beek, P. Foreland Exhumation Controlled by Crustal Thickening in the Western Alps. *Geology* **2017**, *45*, 139–142. [CrossRef]

68. Bernet, M. Detrital Zircon Fission–Track Thermochronology of the Present–Day Isère River Drainage System in the Western Alps: No Evidence for Increasing Erosion Rates at 5 Ma. *Geosciences* **2013**, *3*, 528–542. [CrossRef]
69. Roberts, N.M.; Holdsworth, R.E. Timescales of Faulting through Calcite Geochronology: A Review. *J. Struct. Geol.* **2022**, 104578. [CrossRef]
70. Bilau, A. Ph.D. Thesis, University of Savoie Mont Blanc, Chambéry, Francuska. *in press*.
71. Sue, C.; Tricart, P. Widespread Post–Nappe Normal Faulting in the Internal Western Alps: A New Constraint on Arc Dynamics. *J. Geol. Soc.* **2002**, *159*, 61–70. [CrossRef]
72. Sue, C.; Tricart, P. Neogene to Ongoing Normal Faulting in the Inner Western Alps: A Major Evolution of the Late Alpine Tectonics. *Tectonics* **2003**, *22*. [CrossRef]
73. Mathey, M.; Doin, M.-P.; André, P.; Walpersdorf, A.; Baize, S.; Sue, C. Spatial Heterogeneity of Uplift Pattern in the Western European Alps Revealed by InSAR Time–Series Analysis. *Geophys. Res. Lett.* **2022**, *49*, e2021GL095744. [CrossRef]
74. Champagnac, J. –D.; Schlunegger, F.; Norton, K.; von Blanckenburg, F.; Abbühl, L.M.; Schwab, M. Erosion–Driven Uplift of the Modern Central Alps. *Tectonophysics* **2009**, *474*, 236–249. [CrossRef]
75. Fantoni, R.; Massari, F.; Minervini, M.; Rogledi, S.; Rossi, M. Il Messiniano Del Margine Sudalpino–Padano: Relazioni Tra Contesto Strutturale e Stratigrafico–Deposizionale. *Geol. Insubr.* **2001**, *6*, 95–108.
76. Cazzini, F.; Zotto, O.D.; Fantoni, R.; Ghielmi, M.; Ronchi, P.; Scotti, P. Oil and gas in the Adriatic foreland, Italy. *J. Pet. Geol.* **2015**, *38*, 255–279. [CrossRef]
77. Serpelloni, E.; Faccenna, C.; Spada, G.; Dong, D.; Williams, S.D. Vertical GPS Ground Motion Rates in the Euro–Mediterranean Region: New Evidence of Velocity Gradients at Different Spatial Scales along the Nubia–Eurasia Plate Boundary. *J. Geophys. Res. Solid Earth* **2013**, *118*, 6003–6024. [CrossRef]
78. Becker, A. The Jura Mountains—An Active Foreland Fold–and–Thrust Belt? *Tectonophysics* **2000**, *321*, 381–406. [CrossRef]
79. Bolliger, T.; Engesser, B.; Weidmann, M. Première Découverte de Mammifères Pliocènes Dans Le Jura Neuchâtelois. *Eclogae Geol. Helv.* **1993**, *86*, 1031–1068.
80. Looser, N.; Madritsch, H.; Guillong, M.; Laurent, O.; Wohlwend, S.; Bernasconi, S. Absolute Age and Temperature Constraints on Deformation Along the Basal Décollement of the Jura Fold–and–Thrust Belt from Carbonate U–Pb Dating and Clumped Isotopes. *Tectonics* **2021**, *40*, e2020TC006439. [CrossRef]
81. Smeraglia, L.; Looser, N.; Fabbri, O.; Choulet, F.; Guillong, M.; Bernasconi, S.M. U–Pb Dating of Middle Eocene–Pliocene Multiple Tectonic Pulses in the Alpine Foreland. *Solid Earth* **2021**, *12*, 2539–2551. [CrossRef]
82. Thouvenot, F.; Fréchet, J.; Tapponnier, P.; Thomas, J.-C.; Le Brun, B.; Ménard, G.; Lacassin, R.; Jenatton, L.; Grasso, J.-R.; Coutant, O.; et al. The ML 5.3 Epagny (French Alps) Earthquake of 1996 July 15: A Long–Awaited Event on the Vuache Fault. *Geophys. J. Int.* **1998**, *135*, 876–892. [CrossRef]
83. Baer, M.; Deichmann, N.; Braunmiller, J.; Husen, S.; Fäh, D.; Giardini, D.; Kästli, P.; KRadolfer, U.; Wiemer, S. Earthquakes in Switzerland and Surrounding Regions during 2004. *Eclogae Geol. Helv.* **2005**, *98*, 407–418. [CrossRef]
84. Madritsch, H.; Schmid, S.M.; Fabbri, O. Interactions between Thin– and Thick–Skinned Tectonics at the Northwestern Front of the Jura Fold–and–Thrust Belt (Eastern France). *Tectonics* **2008**, *27*. [CrossRef]
85. Walpersdorf, A.; Hatzfeld, D.; Nankali, H.; Tavakoli, F.; Nilforoushan, F.; Tatar, M.; Vernant, P.; Chéry, J.; Masson, F. Difference in the GPS Deformation Pattern of North and Central Zagros (Iran). *Geophys. J. Int.* **2006**, *167*, 1077–1088. [CrossRef]
86. Ziegler, P.A.; Fraefel, M. Response of Drainage Systems to Neogene Evolution of the Jura Fold–Thrust Belt and Upper Rhine Graben. *Swiss J. Geosci.* **2009**, *102*, 57–75. [CrossRef]
87. Madritsch, H.; Fabbri, O.; Hagedorn, E.-M.; Preusser, F.; Schmid, S.M.; Ziegler, P.A. Feedback between Erosion and Active Deformation: Geomorphic Constraints from the Frontal Jura Fold–and–Thrust Belt (Eastern France). *Int. J. Earth Sci.* **2010**, *99*, 103–122. [CrossRef]
88. Mazzotti, S.; Jomard, H.; Masson, F. Processes and Deformation Rates Generating Seismicity in Metropolitan France and Conterminous Western Europe. *Bull. Soc. Géol. Fr.* **2020**, *191*, 19. [CrossRef]
89. Siame, L.; Bellier, O.; Braucher, R.; Sébrier, M.; Cushing, M.; Bourlès, D.; Hamelin, B.; Baroux, E.; de Voogd, B.; Raisbeck, G.; et al. Local Erosion Rates versus Active Tectonics: Cosmic Ray Exposure Modelling in Provence (South–East France). *Earth Planet. Sci. Lett.* **2004**, *220*, 345–364. [CrossRef]
90. Chardon, D.; Hermitte, D.; Nguyen, F.; Bellier, O. First Paleoseismological Constraints on the Strongest Earthquake in France (Provence) in the Twentieth Century. *Geology* **2005**, *33*, 901–904. [CrossRef]
91. Godard, V.; Hippolyte, J.-C.; Cushing, E.; Espurt, N.; Fleury, J.; Bellier, O.; Ollivier, V.; ASTER Team. Hillslope Denudation and Morphologic Response to a Rock Uplift Gradient. *Earth Surf. Dynam.* **2020**, *8*, 221–243. [CrossRef]
92. Molliex, S.; Bellier, O.; Terrier, M.; Lamarche, J.; Martelet, G.; Espurt, N. Tectonic and Sedimentary Inheritance on the Structural Framework of Provence (SE France): Importance of the Salon–Cavaillon Fault. *Tectonophysics* **2011**, *501*, 1–16. [CrossRef]
93. Thomas, F.; Godard, V.; Bellier, O.; Benedetti, L.; Ollivier, V.; Rizza, M.; Guillou, V.; Hollender, F.; Aumaitre, G.; Bourlès, D.L.; et al. Limited Influence of Climatic Gradients on the Denudation of a Mediterranean Carbonate Landscape. *Geomorphology* **2018**, *316*, 44–58. [CrossRef]
94. Willett, S.D. Late Neogene Erosion of the Alps: A Climate Driver? *Annu. Rev. Earth Planet. Sci.* **2010**, *38*, 411–437. [CrossRef]

95. Sternai, P.; Sue, C.; Husson, L.; Serpelloni, E.; Becker, T.W.; Willett, S.D.; Faccenna, C.; Di Giulio, A.; Spada, G.; Jolivet, L.; et al. Present–Day Uplift of the European Alps: Evaluating Mechanisms and Models of Their Relative Contributions. *Earth-Sci. Rev.* **2019**, *190*, 589–604. [CrossRef]
96. Cederbom, C.E.; van der Beek, P.; Schlunegger, F.; Sinclair, H.D.; Oncken, O. Rapid extensive erosion of the North Alpine foreland basin at 5–4 Ma. *Basin Res.* **2011**, *23*, 528–550. [CrossRef]
97. Glotzbach, C.; Beek, P.; Spiegel, C. Episodic Exhumation and Relief Growth in the Mont Blanc Massif, Western Alps from Numerical Modelling of Thermochronology Data. *Earth Planet. Sci. Lett.* **2011**, *304*, 417–430. [CrossRef]
98. Saillard, M.; Petit, C.; Rolland, Y.; Braucher, R.; Bourlès, D.L.; Zerathe, S.; Revel, M.; Jourdon, A. Late Quaternary Incision Rates in the Vésubie Catchment Area (Southern French Alps) from in Situ–Produced 36Cl Cosmogenic Nuclide Dating: Tectonic and Climatic Implications. *J. Geophys. Res. Earth Surf.* **2014**, *119*, 1121–1135. [CrossRef]
99. Rolland, Y.; Petit, C.; Saillard, M.; Braucher, R.; Bourlès, D.; Darnault, R.; Cassol, D.; Team, A.; ASTER Team. Inner Gorges Incision History: A Proxy for Deglaciation? Insights from Cosmic Ray Exposure Dating (10Be and 36Cl) of River–Polished Surfaces (Tinée River, SW Alps, France). *Earth Planet. Sci. Lett.* **2017**, *457*, 271–281. [CrossRef]
100. Petit, C.; Goren, L.; Rolland, Y.; Bourlès, D.; Braucher, R.; Saillard, M.; Cassol, D. Recent, Climate–Driven River Incision Rate Fluctuations in the Mercantour Crystalline Massif, Southern French Alps. *Quat. Sci. Rev.* **2017**, *165*, 73–87. [CrossRef]
101. Petit, C.; Rolland, Y.; Braucher, R.; Bourlès, D.; Guillou, V.; Petitperrin, V. River Incision and Migration Deduced from 36Cl Cosmic–Ray Exposure Durations: The Clue de La Cerise Gorge in Southern French Alps. *Geomorphology* **2019**, *330*, 81–88. [CrossRef]
102. Mariotti, A.; Blard, P.-H.; Charreau, J.; Petit, C.; Molliex, S.; ASTER Team. Denudation Systematics Inferred from in Situ Cosmogenic 10 Be Concentrations in Fine (50–100 Mm) and Medium (100–250 Mm) Sediments of the Var River Basin, Southern French Alps. *Earth Surf. Dyn.* **2019**, *7*, 1059–1074. [CrossRef]
103. Cardinal, T.; Audin, L.; Rolland, Y.; Schwartz, S.; Petit, C.; Zerathe, S.; Borgniet, L.; Braucher, R.; Nomade, J.; Dumont, T. Interplay of Fluvial Incision and Rockfalls in Shaping Periglacial Mountain Gorges. *Geomorphology* **2021**, *381*, 107665. [CrossRef]
104. Cardinal, T.; Petit, C.; Rolland, Y.; Audin, L.; Schwartz, S.; Valla, P.G.; Zerathe, S.; Braucher, R.; Aster Team. Fluvial bedrock gorges as markers for Late–Quaternary tectonic and climatic forcing in the Southwestern Alps. *Geomorphology* **2022**, *418*, 108476. [CrossRef]
105. Rolland, Y.; Darnault, R.; Braucher, R.; Bourlès, D.; Petit, C.; Bouissou, S.; Team, A. Deglaciation History at the Alpine–Mediterranean Transition (Argentera–Mercantour, SW Alps) from 10Be Dating of Moraines and Glacially Polished Bedrock. *Earth Surf. Processes Landf.* **2020**, *45*, 393–410. [CrossRef]
106. Delunel, R.; Schlunegger, F.; Valla, P.G.; Dixon, J.; Glotzbach, C.; Hippe, K.; Kober, F.; Molliex, S.; Norton, K.P.; Salcher, B. Late–Pleistocene Catchment–Wide Denudation Patterns across the European Alps. *Earth-Sci. Rev.* **2020**, *211*, 103407. [CrossRef]
107. Barruol, G.; Bonnin, M.; Pedersen, H.; Bokelmann, G.H.; Tiberi, C. Belt–parallel mantle flow beneath a halted continental collision: The Western Alps. *Earth Planet. Sci. Lett.* **2011**, *302*, 429–438. [CrossRef]